Volume 6, Issue 6
December 2017

ITEE Journal
Information Technology & Electrical Engineering

ISSN: - 2306-708X

Comparative Study between Sliding Mode Control and Backstepping Control for Double Star Induction Machine (DSIM) under Current Sensor Faults

[1]Noureddine Layadi, [2] Samir Zeghlache, [3] Fouad Berrabah, [4] Larafi Bentouhami

[1] Laboratory of Electrical Engineering, Department of Electrical Engineering, Faculty of Technology, University Mohamed Boudiaf of M'sila, BP 166, Ichbilia 28000, Algeria

[2] Laboratory of Analysis of Signals and Systems, Department of Electronics, Faculty of Technology, University Mohamed Boudiaf of M'sila, BP 166, Ichbilia 28000, Algeria

[3]Department of Electrical Engineering, Faculty of Technology, University Mohamed Boudiaf of M'sila, BP 166, Ichbilia 28000, Algeria

[4] LEB-research laboratory department of electrical engineering, university of batna-2, Algeria

E-mail: [1]masterbba2015@gmail.com, [2]zegsam5@gmail.com, [3]Fouadberrabah1@gmail.com, [4]mecatronic.larafi@gmail.com

ABSTRACT

This paper presents an accurate and high-efficiency backstepping fault-tolerant control (FTC) for double star induction machine (DSIM) of 4,5 kw operating with two current sensor faults (CSFs). The DSIM is fed by two cascaded hybrid seven level inverter using pulse width modulation (PWM) control strategies. This passive FTC is based on Lyapunov stability theory and using an estimator of rotor flux. A comparative analysis via Matlab/Simulink is made between the proposed FTC and sliding mode control (SMC) in order to compare the performances of the system using these two control methods. Simulation results prove that the backstepping FTC has a fast dynamic, better tracking performance and better robustness against the CSFs.

Keywords: *Double star induction machine, Backstepping control, Sliding mode control, Fault tolerant control, Current sensor fault.*

1. INTRODUCTION

The double star induction machine (DSIM) belongs to the multiphase machines category. It has been proposed for different fields of industry that need high power such as electric hybrid vehicles, locomotive traction and ship propulsion and other applications which requires safeness conditions such as aerospace and offshore wind energy systems. DSIM not only guarantees a decrease of rotor harmonics currents and lower torque ripple but it also has many other advantages such as: reliability, power segmentation and higher efficiency. DSIM has a greater fault tolerance; it can continue to operating even with open-phase faults thanks to the important number of phases it owns [1-5].

Sensors are very delicate and can be broken. Current sensor faults (CSFs) are one of the most important concerns in industrial fields. The most widely used method for detecting a current sensor fault is based on Kirchhoff's law. A CSF occurs if the sum of (abc) frame measured phase currents does not equal zero. However, faulty sensors can provoke the instability of DSIM. Moreover several observers like sliding mode, extended kalman filter or neural networks use stator currents signals to estimate rotor flux, electromagnetic torque and rotor speed therefore their estimations will be unreliable when those sensors are faulty [6]. For these reasons it is very important to develop a sensor fault tolerant control able to keep good system performances even under these operating conditions.

In the last few years, fault-tolerant control for induction motor became a very attractive research field for many researchers [7-9]. The aim of the fault tolerant control is having the ability to accommodate automatically when occurrence a fault and to maintain acceptable system performances. In the literature, there are two methods of fault-tolerant control: passive fault-tolerant control (PFTC) and active fault-tolerant control (AFTC). PFTC uses robust control techniques to guarantees the insensitivity of system to faults in closed loop, the system continues to operate with the same controller and system structure [10], in other hand AFTC is based on-line fault compensation. It has the ability to change its structure according to the information provided by the FDI (Fault detection and isolation) block [11]. The complexity of DSIM mathematical model requires the PFTC, in this reason a FTC based on Backstepping control is proposed in this paper.

The sliding mode control (SMC) is a non linear control, it has a fast dynamic response where the system stability is guaranteed by reducing transient state error. The SMC ensures robustness against parameter variation and external disturbance when the system reaches and remains in the sliding surface. In other hand, the SMC present a disadvantage called chattering. This unwanted phenomenon is under high frequency ripples form caused by the switching control law [12-13]. SMC has recently been applied on doubly fed induction generator where it has proved its robustness against parameters variation and disturbances in front of the both proportional-Integral and backstepping control [14-15]. The only disadvantage is the chattering phenomenon. It has also been successfully applied on permanent magnetic synchronous motor (PMSM) where the unpleasant chattering phenomenon was eliminated by using an exponential reaching law [16].

Backstepping control (BSC) is a non linear control based on Lyapunov theory. Recently it has been widely studied and adapted for the control. Researchers in the field of induction

Volume 6, Issue 5October2017

ITEE Journal
Information Technology & Electrical Engineering

ISSN: - 2306-708X

motor (IM) interested by the high efficiency of BSC in stability of closed-loop systems have proposed several process of applying the backstepping control to IM. [17] presents a BSC for induction motor drive using reduced model in healthy state, simulation and experimental results show the good performances of IM under operating in low and inverse speed, they also confirm the high robustness against external disturbance and parameters variations. Backstepping control is equally applied on five phase induction motor drive [18-20]. The experimental tests obtained prove the best performances in transitional and steady state, excellent stability in low speed operation state and robustness against temperature variation (resistance variation), the only disadvantage is the adjustment of gains. The field of wind energy conversion systems (WECS) also took advantage of BSC. In [21] a backstepping control strategy was developed and tested on double fed induction generator (DFIG) for the purpose to control the stator outputs voltage and frequency under perturbations generated by speed and required power variations. Experimental results using a DFIG and a dSpace DS11104 card prove the performances of the proposed control such as precision and stability.

This paper introduces a comparative study of sliding mode and backstepping in control of the double star induction machine. Modeling, theoretical study and simulations are provided. Performance of both controllers is investigated and compared in term of tracking reference, external disturbance and robustness against current sensor fault.

After the introduction, this paper is organized as follows: the next section describe the DSIM and establish the state equations in d-q reference frame. Section 3 simulates the current sensor fault. Sliding mode control design for DSIM is carried out in section 4. Backstepping control scheme is developed in section 5. The proposed FTC is implemented in Matlab/Simulink environment and performance appraisal is examined in Section 6. The last section is reserved for conclusion.

2. DSIM MODELLING

2.1. DSIM DESCRIPTION

The DSIM has two stators shifted by an electrical angle and mobile squirrel cage rotor composed by three phases. Each star is composed by three immovable windings. The Fig. 1 shows an explicit schema which represents the stator and rotor windings. The windings series (S_{a1}, S_{b1}, S_{c1}), (S_{a2}, S_{b2}, S_{c2}) , (R_a, R_b, S_c) represent stator1, stator2 and rotor respectively, α is the angle shift between the two stators, θ is the one between rotor and stator1. In this research we choose α=30° as [3]. In order to have a light mathematical model of DSIM, we are putting these assumptions:

- The two stators are identical.
- The windings are sinusoidal distributed.
- The magnetic saturation and mutual leakage are neglected.
- The flux path is linear.

2.2. DSIM State equations

From the hypotheses cited above and in order to design easily the proposed backstepping controller, we choose the following state space model of DSIM in the synchronously rotating reference frame (d-q):

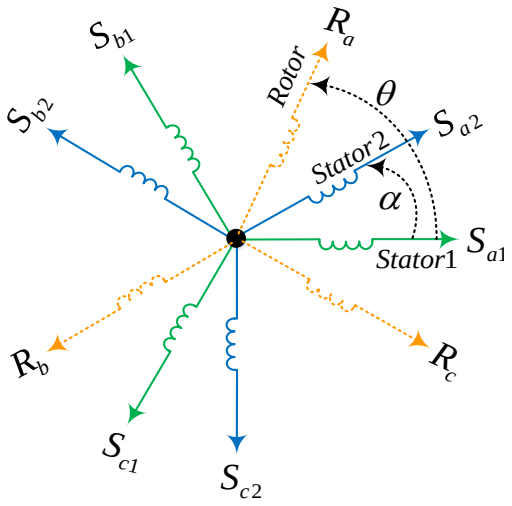

Fig.1 DSIM windings

$$\frac{d}{dt}i_{sd1} = \frac{1}{L_{s1}}[v_{sd1} - R_{s1}i_{sd1} + \omega_s^*(L_{s1}i_{sq1} + T_r\varphi_r^*\omega_{gl}^*)] \quad (1)$$

$$\frac{d}{dt}i_{sq1} = \frac{1}{L_{s1}}[v_{sq1} - R_{s1}i_{sq1} - \omega_s^*(L_{s1}i_{sd1} + \varphi_r^*)] \quad (2)$$

$$\frac{d}{dt}i_{sd2} = \frac{1}{L_{s2}}[v_{sd2} - R_{s2}i_{sd2} + \omega_s^*(L_{s2}i_{sq2} + T_r\varphi_r^*\omega_{gl}^*)] \quad (3)$$

$$\frac{d}{dt}i_{sq2} = \frac{1}{L_{s2}}[v_{sq2} - R_{s2}i_{sq2} - \omega_s^*(L_{s2}i_{sd2} + \varphi_r^*)] \quad (4)$$

$$\frac{d}{dt}\omega_r = \frac{1}{J}\left[p^2\frac{L_m}{L_m + L_r}\varphi_r^*(i_{sq1} + i_{sq2}) - pT_L - K_f\omega_r\right] \quad (5)$$

$$\frac{d}{dt}\varphi_r = -\frac{R_r}{L_m + L_r}\varphi_r + \frac{L_m R_r}{L_m + L_r}(i_{sd1} + i_{sd2}) \quad (6)$$

3. SIMULATION OF CURRENT SENSOR FAULT IN MATLAB/SIMULINK

This simulation method is based on the stator current transformation from abc frame to the stationary reference frame (alpha-beta) as shown in Fig. 2. Current components $i_{s\alpha}$ and $i_{s\beta}$ can be calculated from the following system of equations [10]:

$$\begin{cases} i_{s\alpha} = i_{sa} \\ i_{s\beta} = \frac{\sqrt{3}}{3}(i_{sa} + 2i_{sb}) \end{cases} \quad (7)$$

Two current sensor faults were introduced in control loop with both stators by multiplying the two current signals $i_{s\alpha1}$ and $i_{s\alpha2}$ By an error gain as indicated in Fig. 3.

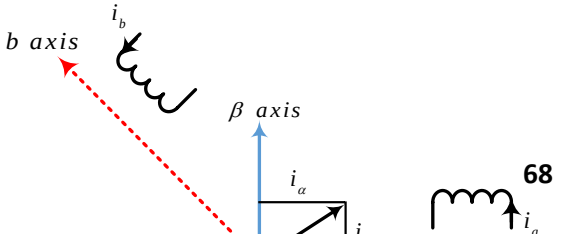

Volume 6, Issue 5October2017

ITEE Journal
Information Technology & Electrical Engineering

ISSN: - 2306-708X

4. SLIDING MODE CONTROL DESIGN

4.1. SLIDING MODE THEORY [22]

The sliding mode control is based on the convergence of system state trajectory to a sliding surface. The state vector is kept around this surface by the switching control effort in order that the trajectory slides to the origin through the sliding surface. The design of SMC can be reach in two successive steps:

- **First step:** definition of sliding surfaces

The most used surface S(x) in the literature is given by:

$$S(t) = \left(\lambda + \frac{d}{dt}\right)^{r-1} (x_{ref} - x) \quad (8)$$

Where x is the state vector, x_{ref} is the reference state vector, r is the degree of the sliding mode and λ is the weighting factor.

$$u(t) = u_{eq}(t) + u_N(t) \quad (9)$$

The component u_{eq} called the equivalent control (decoupling control) is obtained by putting surface derivate equals zero $\dot{S}(t) = 0$, its role is holding the system on the sliding surface which is definite by $S(t) = 0$. The other constituent u_N is the discontinuous control (switching control) it ensures the convergence of system state trajectory toward sliding surface. The reaching condition is based on Lyapunov theory stability and must verify $\dot{S}.S < 0$.

4.2. APPLICATION OF SMC ON DSIM:

The SMC algorithm for DSIM has been presented in [23-24]. In order to eliminate or decrease the chattering phenomena in steady state, a saturation function sat(t) is used instead the signum function sgn(t) for the switching control [25]. The sat(t) function is defined as [26]:

$$sat(t) = \frac{S}{|s| + m} \quad (10)$$

Where m is a small positive gain and $|S| >> m$.

Therefore, the SMC for DSIM can be designed as follows:

- **Speed and flux SMC:**

Speed and flux surface:

$$\begin{cases} s(\omega_r) = \omega^* - \omega \\ s(\varphi_r) = \varphi^* - \varphi \end{cases} \quad (11)$$

The time derivative of equation (11) gives:

$$\begin{cases} \dot{S}(\omega_r) = \dot{\omega}_r^* - \dot{\omega}_r \\ \dot{S}(\omega_r) = \dot{\varphi}_r^* - \dot{\varphi}_r \end{cases} \quad (12)$$

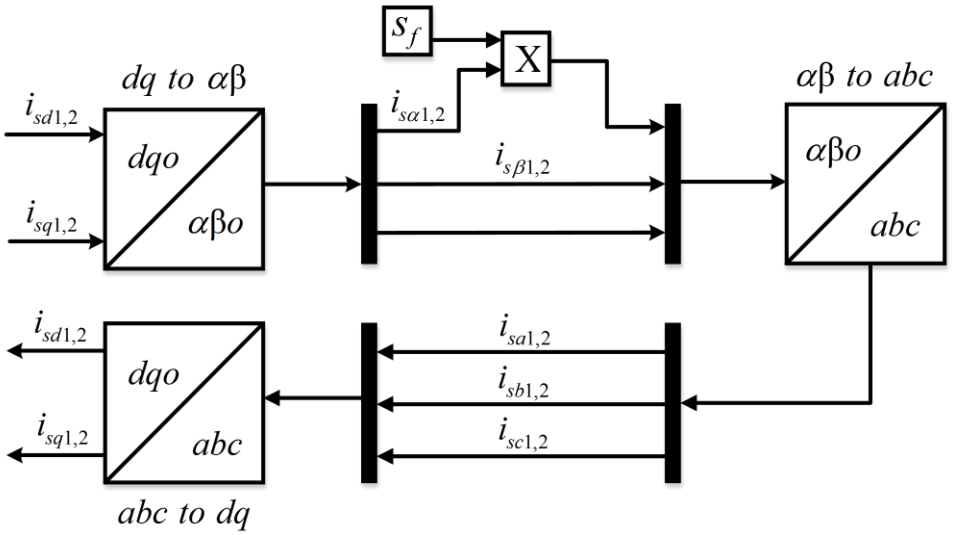

Fig.3 Simulation of current sensor fault (S_f is a gain error: 20% of the nominal signal)

- **Second step:** Control law design

The sliding mode control has two command components and can be written as follows:

Volume 6, Issue 5October2017

ITEE Journal
Information Technology & Electrical Engineering

ISSN: - 2306-708X

By substituting equations (5) and (6) into (12) we get:

$$\begin{cases} \dot{S}(\omega_r) = \dot{\omega}_r^* - \dfrac{p^2}{J}\dfrac{L_m}{L_m + L_r}(i_{sq1} + i_{sq2})\varphi_r^* - \dfrac{K_f}{J}\omega_r - \dfrac{p}{J}T_L \\ \dot{S}(\varphi_r) = \dot{\varphi}_r^* + \dfrac{R_r}{L_m + L_r}\varphi_r - \dfrac{L_m R_r}{L_m + L_r}(i_{sd1} + i_{sd2}) \end{cases} \quad (13)$$

Assuming that:

$$\begin{cases} i_{sd1} + i_{sd2} = i_{sd} \\ i_{sq1} + i_{sq2} = i_{sq} \\ i_{sd1} = i_{sd2} \\ i_{sq1} = i_{sq2} \end{cases} \quad (14)$$

And putting:

$$\begin{cases} i_{sq} = i_{sq}^* = i_{sqeq} + i_{sqn} \\ i_{sd} = i_{sd}^* = i_{sdeq} + i_{sdn} \end{cases} \quad (15)$$

Using equations (13), (14) and (15) we obtain:

$$\dot{S}(\omega_r) = \dot{\omega}_r^* - \frac{p^2}{J}\frac{L_m}{L_m + L_r}\varphi_r^* i_{sqeq} - \frac{p^2}{J}\frac{L_m}{L_m + L_r}\varphi_r^* i_{sqn} + \frac{K_f}{J}\omega_r + \frac{p}{J}T_L \quad (16)$$

By applying the SMC theory, we find the d-q axis components of currents control:

$$\begin{cases} i_{sdeq} = \dfrac{L_m + L_r}{R_r L_m}\left[\varphi_r^* + \dfrac{R_r}{L_m + L_r}\varphi_r\right] \\ i_{sqeq} = \dfrac{J}{p^2}\dfrac{L_m + L_r}{L_m}\varphi_r^*\left[\dot{\omega}_r^* + \dfrac{K_f}{J}\omega_r + \dfrac{p}{J}T_L\right] \\ i_{sdn} = k_{\varphi_r}\dfrac{S(\varphi_r)}{|S(\varphi_r)| + m_{\varphi_r}} \\ i_{sqn} = k_{\omega_r}\dfrac{S(\omega_r)}{|S(\omega_r)| + m_{\omega_r}} \end{cases} \quad (17)$$

Where k_{φ_r} and k_{ω_r} are positive constants

- **Currents SMC:**

Currents surface:

$$\begin{cases} s(i_{sd1}) = i_{sd1}^* - i_{sd1} \\ s(i_{sq1}) = i_{sq1}^* - i_{sq1} \\ s(i_{sd2}) = i_{sd2}^* - i_{sd2} \\ s(i_{sq2}) = i_{sq2}^* - i_{sq2} \end{cases} \quad (18)$$

The derivative of equation (18) according the time gives:

$$\begin{cases} S(i_{sd1}) = \dfrac{d}{dt}i_{sd1}^* - \dfrac{d}{dt}i_{sd1} \\ S(i_{sq1}) = \dfrac{d}{dt}i_{sq1}^* - \dfrac{d}{dt}i_{sq1} \\ S(i_{sd2}) = \dfrac{d}{dt}i_{sd2}^* - \dfrac{d}{dt}i_{sd2} \\ S(i_{sq2}) = \dfrac{d}{dt}i_{sq2}^* - \dfrac{d}{dt}i_{sq2} \end{cases} \quad (19)$$

By using equations (1), (2), (3) and (4) the system of equations (19) became:

$$\dot{S}\left(\frac{d}{dt}i_{sd1}\right) = i_{sd1}^* - \frac{1}{L_{s1}}(v_{sd1} - R_{s1}i_{sd1}) + \frac{1}{L_{s1}}[\omega_s^*(L_{s1}i_{sq1} + T_r\varphi_r^*\omega_{gl}^*)] \quad (20)$$

$$\dot{S}\left(\frac{d}{dt}i_{sq1}\right) = i_{sq1}^* - \frac{1}{L_{s1}}(v_{sq1} - R_{s1}i_{sq1}) - \frac{1}{L_{s1}}[\omega_s^*(L_{s1}i_{sd1} + \varphi_r^*)] \quad (21)$$

$$\dot{S}\left(\frac{d}{dt}i_{sd2}\right) = i_{sd2}^* - \frac{1}{L_{s2}}(v_{sd2} - R_{s2}i_{sd2}) + \frac{1}{L_{s2}}[\omega_s^*(L_{s2}i_{sq2} + T_r\varphi_r^*\omega_{gl}^*)] \quad (22)$$

$$\dot{S}\left(\frac{d}{dt}i_{sq2}\right) = i_{sq2}^* - \frac{1}{L_{s2}}(v_{sq2} - R_{s2}i_{sq2}) - \frac{1}{L_{s2}}[\omega_s^*(L_{s2}i_{sd2} + \varphi_r^*)] \quad (23)$$

Putting:

$$\begin{cases} v_{sd1} = v_{sd1}^* = v_{sd1eq} + v_{sd1n} \\ v_{sq1} = v_{sq1}^* = v_{sq1eq} + v_{sq1n} \\ v_{sd2} = v_{sd2}^* = v_{sd2eq} + v_{sd2n} \\ v_{sq2} = v_{sq2}^* = v_{sq2eq} + v_{sq2n} \end{cases} \quad (24)$$

Finally, by following the same method used with the currents sliding mode control, we get the decoupling control voltages:

$$\begin{cases} v_{sd1eq} = L_{s1}\dfrac{d}{dt}i_{sd1}^* + R_{s1}i_{sd1} - \omega_s^*(L_{s1}i_{sq1} + T_r\varphi_r^*\omega_{gl}^*) \\ v_{sq1eq} = L_{s1}\dfrac{d}{dt}i_{sq1}^* + R_{s1}i_{sq1} + \omega_s^*(L_{s1}i_{sd1} + \varphi_r^*) \\ v_{sd2eq} = L_{s2}\dfrac{d}{dt}i_{sd2}^* + R_{s2}i_{sd2} - \omega_s^*(L_{s2}i_{sq2} + T_r\varphi_r^*\omega_{gl}^*) \\ v_{sq2eq} = L_{s2}\dfrac{d}{dt}i_{sq2}^* + R_{s2}i_{sq2} + \omega_s^*(L_{s2}i_{sd2} + \varphi_r^*) \end{cases} \quad (25)$$

And also the switching control voltages:

$$\begin{cases} v_{sd1n} = k_{sd1}\dfrac{S(i_{sd1})}{|S(i_{sd1})| + m_{sd1}} \\ v_{sq1n} = k_{sq1}\dfrac{S(i_{sq1})}{|S(i_{sq1})| + m_{sq1}} \\ v_{sd2n} = k_{sd2}\dfrac{S(i_{sd2})}{|S(i_{sd2})| + m_{sd2}} \\ v_{sq2n} = k_{sq2}\dfrac{S(i_{sq2})}{|S(i_{sq2})| + m_{sq2}} \end{cases} \quad (26)$$

Where k_{sd1}, k_{sq1}, k_{sd2} and k_{sq2} are positive gains that stabilize the closed-loop system and obtained by adjustment.

5. BACKSTEPPING CONTROL DESIGN

Backstepping control design is split into several design steps. The output of each step will be the reference for the next subsystem. The global system stability and performance are confirmed by Lyapunov theory [27]. The BSC scheme for

Volume 6, Issue 5October2017

ITEE Journal
Information Technology & Electrical Engineering

ISSN: - 2306-708X

DSIM with faulty sensors is represented by Fig. 4, in this work the sensors faults effects can be overcome using BSC strategy in two consecutive steps.

- **First step:** speed and flux control

The goal of this step is to steer the vector $[\omega_r \quad \varphi_r]^T$ to its desired reference $[\omega_r \quad \varphi_r]^T$. The tracking errors of speed and flux are given by:

$$\begin{bmatrix} e_1 \\ e_2 \end{bmatrix} = \begin{bmatrix} \omega_r^* - \omega_r \\ \varphi_r^* - \varphi_r \end{bmatrix} \quad (27)$$

The dynamics of tracking errors are:

$$\begin{bmatrix} \dot{e}_1 \\ \dot{e}_2 \end{bmatrix} = \begin{bmatrix} \dot{\omega}_r^* - \dot{\omega}_r \\ \dot{\varphi}_r^* - \dot{\varphi}_r \end{bmatrix} \quad (28)$$

By substituting equations (5) and (6) into system of equations (28), the dynamics of tracking errors became:

$$\begin{bmatrix} \dot{e}_1 \\ \dot{e}_2 \end{bmatrix} = \begin{bmatrix} \dot{\omega}_r^* - \frac{1}{J}\left[p^2 \frac{L_m}{L_m + L_r} \varphi_r^* (i_{sq1} + i_{sq2}) - pT_L - K_f \right] \\ \dot{\varphi}_r^* - \left[-\frac{R_r}{L_m + L_r} \varphi_r + \frac{L_m R_r}{L_m + L_r} (i_{sd1} + i_{sd2}) \right] \end{bmatrix} \quad (29)$$

The first Lyapunov function adaptive to the rotor flux and speed errors is presented by:

$$V_1 = \frac{(e_1^2 + e_2^2)}{2} \quad (30)$$

The dynamic of Lyapunov function is:

$$\dot{V}_1 = e_1 \dot{e}_1 + e_2 \dot{e}_2 \quad (31)$$

From equation (29), $\dot{V}_1$ can be written as follows:

$$\dot{V}_1 = e_1 \left[\dot{\omega}_r^* - \left(\frac{1}{J} p^2 \frac{L_m}{L_m + L_r} \varphi_r^* (i_{sq1} + i_{sq2}) - pT_L - K_f \right) \right] + e_2 \left[\dot{\varphi}_r^* - \left(-\frac{R_r}{L_m + L_r} \varphi_r + \frac{L_m R_r}{L_m + L_r} (i_{sd1} + i_{sd2}) \right) \right] \quad (32)$$

For the purpose to make the Lyapunov function derivative negative definite we choose:

$$\begin{cases} \dot{e}_1 = -G_1 e_1 \\ \dot{e}_2 = -G_2 e_2 \end{cases} \quad (33)$$

Where: G_1, G_2 are positive gains. By replacing system of equations (33) into system of equations (31) the stability is verified by the following inequality:

$$\dot{V}_1 = -G_1 e_1^2 - G_2 e_2^2 < 0 \quad (34)$$

From system of equations (29) and (33) we can make this equality:

$$\begin{cases} \dot{\omega}_r^* - \left(\frac{1}{J} p^2 \frac{L_m}{L_m + L_r} \varphi_r^* (i_{sq1} + i_{sq2}) - pT_L - K_f \right) = -G_1 e_1 \\ \dot{\varphi}_r^* - \left(-\frac{R_r}{L_m + L_r} \varphi_r + \frac{L_m R_r}{L_m + L_r} (i_{sd1} + i_{sd2}) \right) = -G_2 e_2 \end{cases} \quad (35)$$

Putting:

$$\begin{cases} i_{sq1} + i_{sq2} = i_{sq}^* \\ i_{sd1} + i_{sd2} = i_{sd}^* \end{cases} \quad (36)$$

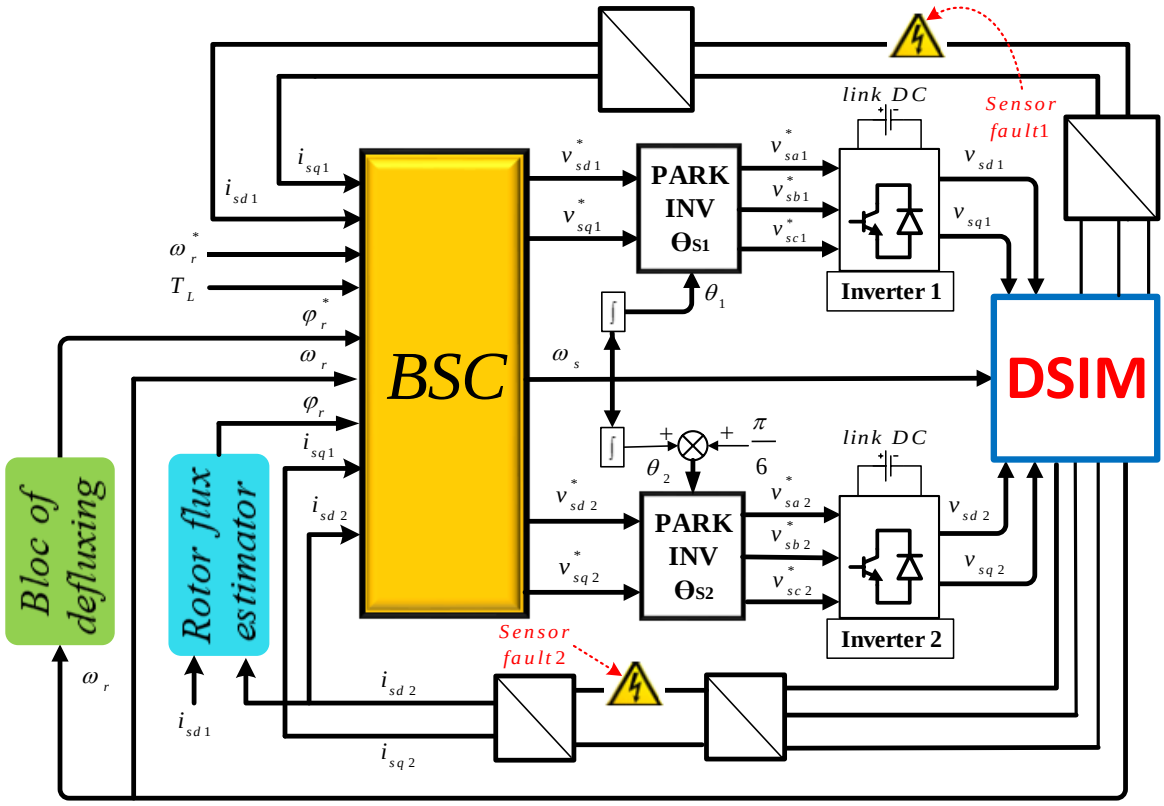

Fig.4 Backstepping control for DSIM affected by two sensor faults

Volume 6, Issue 5October2017

ITEE Journal
Information Technology & Electrical Engineering

ISSN: - 2306-708X

And assuming that:

$$\begin{cases} i_{sq1} = i_{sq2} \\ i_{sd1} = i_{sd2} \end{cases} \quad (37)$$

By substituting system of equations (36) into (35), we find the current control:

$$\begin{cases} i_{sd}^{*} = \dfrac{L_m + L_r}{L_m R_r}\left[\dot{\varphi}_r^{*} + \dfrac{R_r}{L_m + L_r}\varphi_r + G_2 e_2\right] \\ i_{sq}^{*} = \dfrac{J\,(L_m + L_r)}{p^2 L_m \varphi_r^{*}}\left[\dot{\omega}_r^{*} + \dfrac{K_f}{J}\omega_r + \dfrac{p}{J}T_L + G_1 e_1\right] \end{cases} \quad (38)$$

- **Second step:** currents control

This step establish the control law by adjusting the currents $i_{sd1}, i_{sd2}, i_{sq1}$ and i_{sq2} resulted from the first step. The tracking errors of the currents are:

$$\begin{cases} e_3 = i_{sd1}^{*} - i_{sd1} \\ e_4 = i_{sq1}^{*} - i_{sq1} \\ e_5 = i_{sd2}^{*} - i_{sd2} \\ e_6 = i_{sq2}^{*} - i_{sq2} \end{cases} \quad (39)$$

The time derivative of equations (39) gives:

$$\begin{cases} \dot{e}_3 = \dfrac{d}{dt}i_{sd1}^{*} - \dfrac{d}{dt}i_{sd1} \\ \dot{e}_4 = \dfrac{d}{dt}i_{sq1}^{*} - \dfrac{d}{dt}i_{isq1} \\ \dot{e}_5 = \dfrac{d}{dt}i_{sd2}^{*} - \dfrac{d}{dt}i_{sd2} \\ \dot{e}_6 = \dfrac{d}{dt}i_{sq2}^{*} - \dfrac{d}{dt}i_{sq2} \end{cases} \quad (40)$$

By substituting $\frac{d}{dt}i_{sd1}, \frac{d}{dt}i_{sq1}, \frac{d}{dt}i_{sd2}$ and $\frac{d}{dt}i_{sq2}$ by their expressions (1), (2), (3) and (4), the system of equations (40) becomes:

$$\begin{bmatrix} \dot{e}_3 \\ \dot{e}_4 \\ \dot{e}_5 \\ \dot{e}_6 \end{bmatrix} = \begin{bmatrix} i_{sd1}^{*} - \dfrac{1}{L_{s1}}[v_{sd1} - R_{s1}i_{sd1} + \omega_s^{*}(L_{s1}i_{sq1} + T_r\varphi_r^{*}\omega_{gl}^{*})] \\ i_{sq1}^{*} - \dfrac{1}{L_{s1}}[v_{sq1} - R_{s1}i_{sq1} - \omega_s^{*}(L_{s1}i_{sd1} + \varphi_r^{*})] \\ i_{sd2}^{*} - \dfrac{1}{L_{s2}}[v_{sd2} - R_{s2}i_{sd2} + \omega_s^{*}(L_{s2}i_{sq2} + T_r\varphi_r^{*}\omega_{gl}^{*})] \\ i_{sq2}^{*} - \dfrac{1}{L_{s2}}[v_{sq2} - R_{s2}i_{sq2} - \omega_s^{*}(L_{s2}i_{sd2} + \varphi_r^{*})] \end{bmatrix} \quad (41)$$

The global Lyapunov function which analysis the system stability is defined by:

$$V_2 = \frac{(e_1^2 + e_2^2)}{2} + \frac{(e_3^2 + e_4^2 + e_5^2 + e_6^2)}{2} \quad (42)$$

Its time derivative is:

$$\dot{V}_2 = -G_1 e_1^2 - G_2 e_2^2 + \dot{e}_3 e_3 + \dot{e}_4 e_4 + \dot{e}_5 e_5 + \dot{e}_6 e_6 \quad (43)$$

The system global stability is achieve if only $\dot{V}_2$ is definite negative therefore $\dot{e}_3, \dot{e}_4, \dot{e}_5$ and $\dot{e}_6$ are chosen as in the first step:

$$\begin{cases} \dot{e}_3 = -G_3 e_3 \\ \dot{e}_4 = -G_4 e_4 \\ \dot{e}_5 = -G_5 e_5 \\ \dot{e}_6 = -G_6 e_6 \end{cases} \quad (44)$$

Where G_3, G_4, G_5 and G_6 are positives gains that stabilize the system in closed-loop. By substituting system of equations (44) into (43) $\dot{V}_2$ became:

$$\dot{V}_2 = -G_1 e_1^2 - G_2 e_2^2 - G_3 e_3^2 - G_4 e_4^2 - G_5 e_5^2 - G_6 e_6^2 < 0 \quad (45)$$

We show clearly that the system of equations (44) checks the stability according to the Lyapunov theory. By using systems of equations (41) and (44) we obtain the final control represented by the following components of stator voltages:

$$v_{sd1} = L_{s1}\frac{d}{dt}i_{sd1}^{*} + R_{s1}i_{sd1} - \omega_s(L_{s1}i_{sq1} + T_r\varphi_r^{*}\omega_{gl}^{*}) + G_3 e_3 \quad (46)$$

$$v_{sq1} = L_{s1}\frac{d}{dt}i_{sq1}^{*} + R_{s1}i_{sq1} + \omega_s(L_{s1}i_{sd1} + \varphi_r^{*}) + G_4 e_4 \quad (47)$$

$$v_{sd2} = L_{s2}\frac{d}{dt}i_{sd2}^{*} + R_{s2}i_{sd2} - \omega_s(L_{s2}i_{sq2} + T_r\varphi_r^{*}\omega_{gl}^{*}) + G_5 e_5 \quad (48)$$

$$v_{sq2} = L_{s2}\frac{d}{dt}i_{sq2}^{*} + R_{s2}i_{sq2} + \omega_s(L_{s2}i_{sd2} + \varphi_r^{*}) + G_6 e_6 \quad (49)$$

6. SIMULATION RESULTS AND COMPARISONS

In order to verify the effectiveness and robustness of the proposed control compared to sliding mode control especially in faulty operation, two current sensor faults was introduced on both control structure. The DSIM studied in this paper is fed by two cascaded H-bridge 7-level inverter, its parameters are follows: Voltage: 230-380 V, power: 4.5 kw, frequency f=50 Hz. The nominal electrical and mechanical parameters are given in appendix 1. The reference speed is fixed to 200 rd/s. The DSIM is starting in balanced operation, a load torque (14 N.m) is applied at t=2sec and followed by injection of two current sensor faults which occur at the same time t=3sec. This test is done by simulation using Matlab/Simulink environment.

6.1. PRE-FAULT: HEALTHY OPERATING

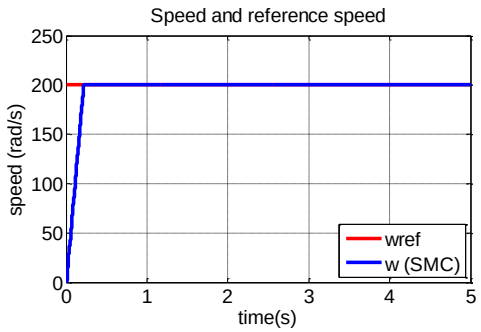

(a)

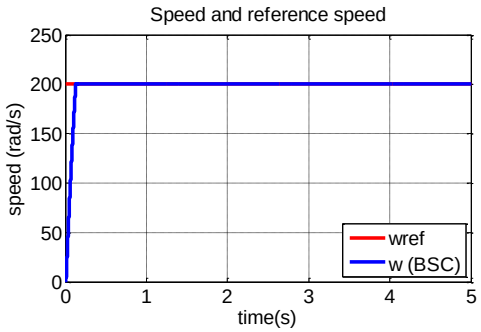

(b)

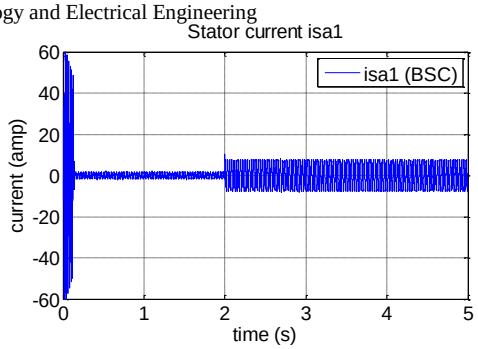

(f)

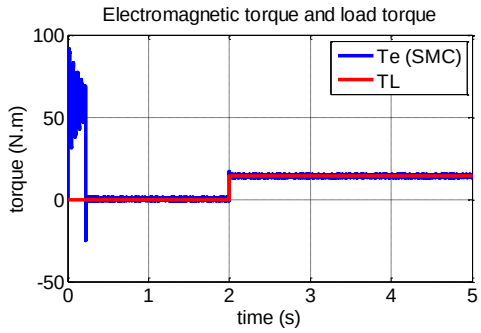

(c)

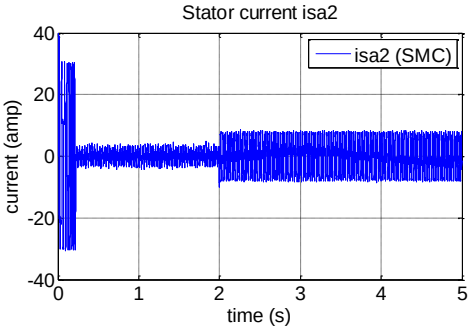

(g)

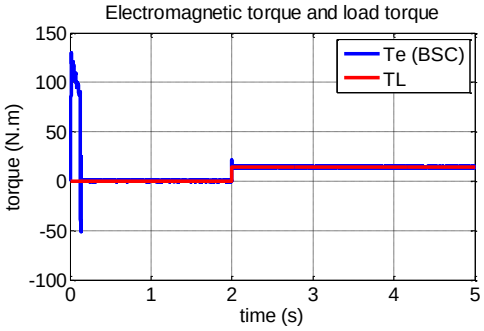

(d)

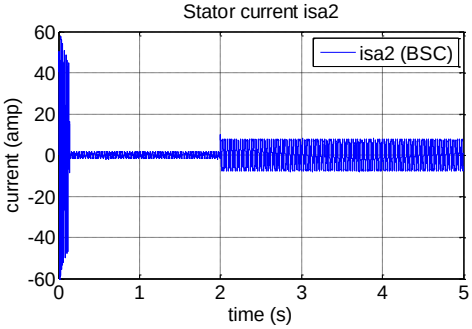

(h)

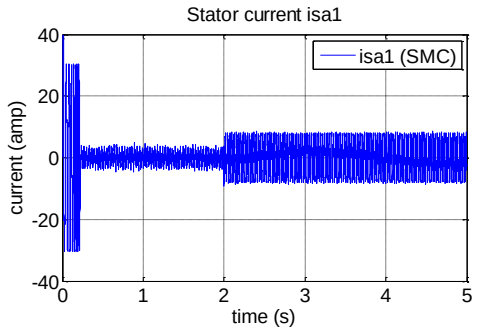

(e)

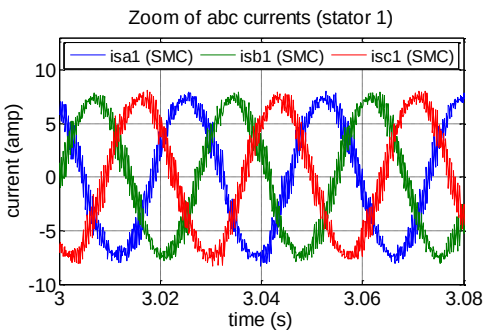

(i)

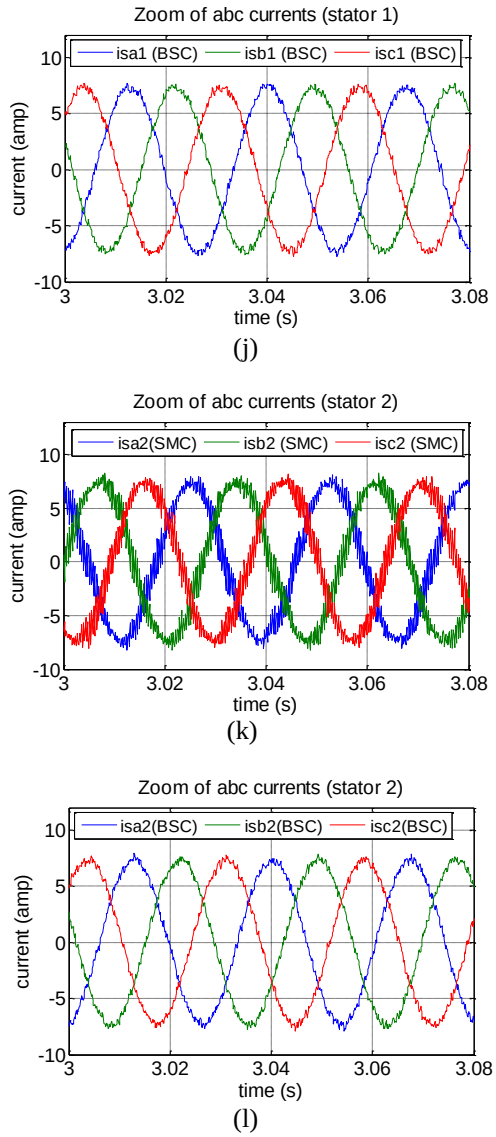

Fig.5 Simulation results of SMC and BSC in healthy state

The Fig. 5 shows the performances of the system in steady and transient-states for a balanced DSIM (un-faulty operation) starting by SMC in the top side and the non linear BSC based on Lyapunov theory in the bottom side for each physical size. Fig. 5.a and Fig. 5.b show the speed responses for the two control methods, in both signals the speed follows its reference value with neglected surpass and without ripples, but it is clearly that the BSC has a faster response that SMC and imposes a short transient regime. The response time for SMC is 0.22 sec while with the proposed control it decreases to 0.13 sec. No ripples in the electromagnetic signals as indicated by Fig. 5.c and Fig. 5.d proving that the two control scheme able to compensate the external load torque effect. We notice also that BSC has a faster dynamic in electromagnetic torque response than SMC. The shapes from Fig. 5.e to Fig. 5.l show the behavior of the three currents abc for each stator. These signals are sinusoidal affected by the switching frequency generated by the inverters, with BSC they are more perfect sinusoidal form. Figures from Fig. 5.i until Fig. 5.l clearly show that the ripples (harmonics) in stator current with SMC are higher than with BSC. The obtained results in a pre-fault state summarize and reflect the responses swiftness of BSC compared to SMC.

6.1. POST-FAULT: CURRENT SENSOR FAULT CASE

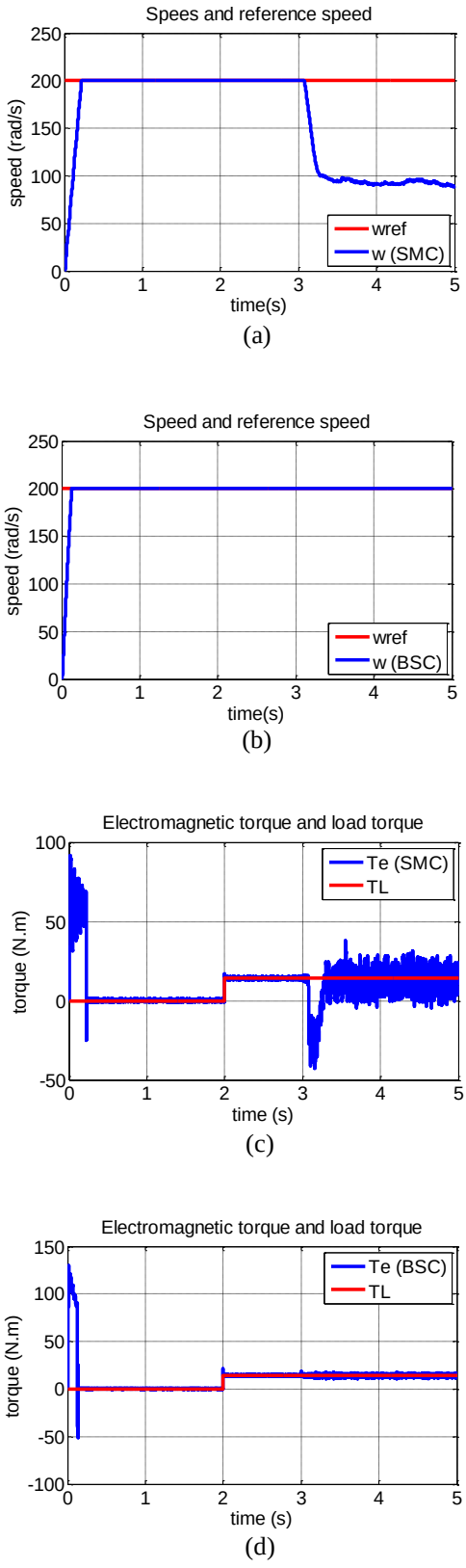

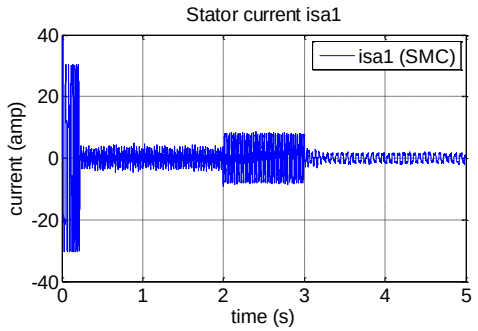

(e)

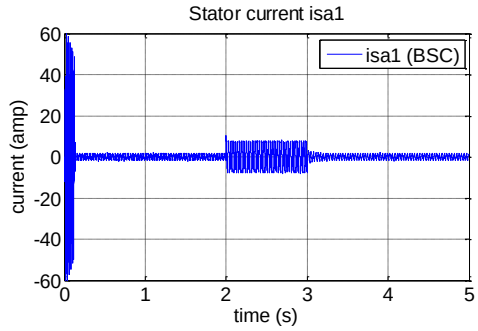

(f)

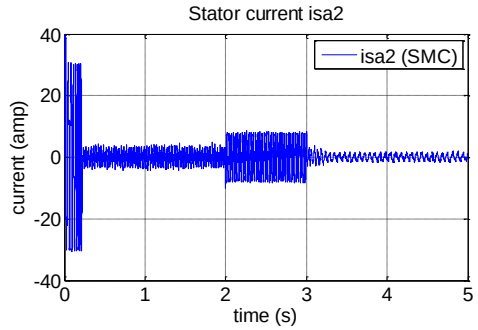

(g)

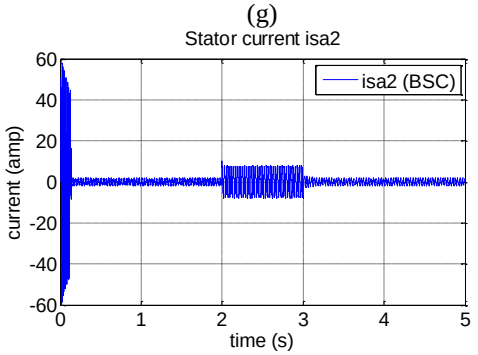

(h)

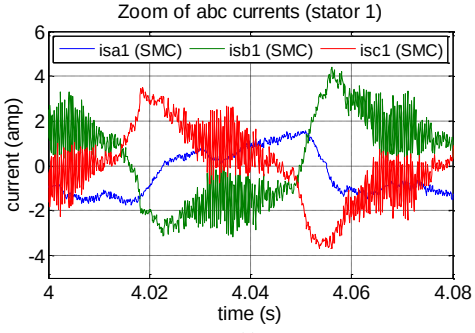

(i)

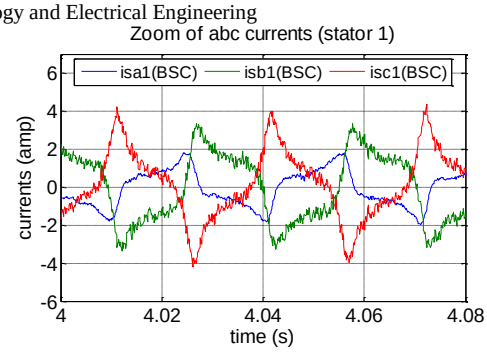

(j)

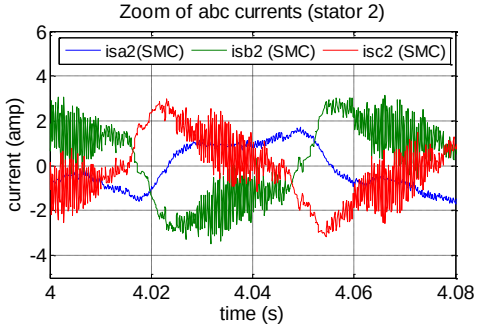

(k)

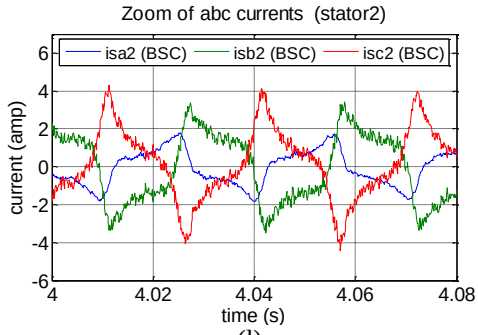

(l)

Fig.6 Simulation results of SMC and BSC with two defective current sensors

In this case the two current sensor faults are created at the same time t=3sec, those faults are immediately detected. The performances of DSIM during post–fault operation are shown in Fig. 6. The machine is driven at 200 rd/s before and after the faults occurrence, with a constant load torque of 14 N.m. In steady state after the faults occur the speed decreases from 200 rd/s to 100 rd/s with SMC method as shown in Fig. 6.a, in the other side the backstepping control retain a good tracking of reference speed. In Fig. 6.c a high ripples in the electromagnetic torque can be view with SMC where the maximum positive ripple reaches +38 N.m and the maximum negative ripple reached -43 N.m but with the proposed control the ripples amplitude is acceptable. During the fault the stator currents in phase S_{a1} and phase S_{a2} decrease with the decrease in the measurements of the stator sensors as shown in Fig. 6.e, Fig .6.f, Fig. 6.g and Fig. 6.h. The sensor faults have also a negative effect on the two currents with healthy sensors of stator1 and stator2 respectively. The deformation of these currents is clearly shown by the zoom-in presented in Fig. 6.i, Fig .6.j, Fig .6.k and Fig. 6.l, this expresses the unbalance of stators

windings. It can be seen from these simulation results that the backstepping control ensures satisfactory robustness against the current sensor faults. On the other hand the SMC is unable to control the unbalanced machine.

7. CONCLUSION

In this paper, a fault tolerant control is presented for double star induction machine affected by two defective current sensors. These sensor faults are injected basing on simple mathematical relationship between currents in phases (a, b, c) and stator current components in stationary reference frame (alpha, beta). The simulation results presented in this paper prove the high efficiency and robustness of the proposed control scheme after the occurrence of current sensor faults compared to sliding mode method. Backstepping control not only gives a higher dynamic and an excellent stability but it can also offers good performances during the faulty operating mode such as good reference speed tracking and satisfactory electromagnetic torque response.

Appendix 1

Table 1. Machine parameters

Parameters	Identifiers & values
Stators resistances	$R_{s1}=R_{s2}=3.72\ \Omega$
Rotor resistance	$R_r=2.12\ \Omega$
Stator self inductances	$L_{s1}=L_{s2}=0.022$ H
Rotor self inductance	$L_{s1}=0.006$ H
Mutual inductance	$L_m=0.3672$ H
Moment of inertia	$J=0.0625$ kg.m^2
Viscous friction coefficient	$K_f=0.001$ Nm.(rd/s)$^{-1}$

REFERENCES

[1] I. Kortas, A. Sakly and M. F. Mimouni, "Optimal Vector Control to a Double star Induction Motor", Energy, vol.131, pp.279-288, 2017.

[2] A. Meroufel, S. Massoum, A. Bentaallah, P. Wira, F. Z. Belaimeche and A. Massoum, "Double Star Induction Motor Direct Torque Control with Fuzzy Sliding Mode Speed Controller", Rev. Roum. Sci. Techn.-Électrotechn. Et Énerg., vol.62, No.1, pp.26-35, 2017.

[3] H. Rahali, S. Zeghlache and L. Benalia, "Adaptive Field-Oriented Control using Supervisory Type-2 Fuzzy Control for Dual Star Induction Machine", International Journal of Intelligent Engineering and Systems, vol.10, No.4, pp.28-40, 2017.

[4] L. Bentouhami, R. Abdessemed, Y. Bendjeddou and E. Merabet, "Neuro-Fuzzy Control of a Dual Star Induction Machine", Journal of Electrical Engineering, vol.16, No.4, pp.1-8, 2016.

[5] Z. Tir, Y. Soufi, M. N. Hashemnia, O.P. Malik and K. Marouani, "Fuzzy Logic Field Oriented Control of Double Star Induction Motor Drive", Electrical Engineering, vol.99, No.2, pp.495-503, 2017.

[6] Y. Yu, Z. Wang, D. Xu, T. Zhou and R. Xu, "Speed and current sensor fault detection and isolation based on adaptive observers for IM drives", Journal of Power Eletronics, vol.14, No.5, pp.967-979, 2014.

[7] M. Manohar and S. Das, "Current Sensor Fault-Tolerant Control for Direct Torque Control of Induction Motor Drive Using Flux Linkage Observer", IEEE Transactions on Industrial Informatics, vol.PP, No.99, pp.1-1, 2017.

[8] Z. Peng, Z. Zheng, Y. Li and Z. Liu, "Fault-tolerant control of multiphase induction machine drives based on virtual winding method", Proceedings of the IEEE Transportation Electrification Conference and Expo, Chicago, IL, USA, pp.252-256, 2017.

[9] Y. Yu, Y. Zhao, B. Wang, X, Huang and D. G. Xu, "Current Sensor Fault Diagnosis and Tolerant Control for VSI-Based Induction Motor Drives", IEEE Transactions on Power Electronics, vol.PP, No.99, pp.1-1, 2017.

[10] K. Klimkowski, "An artificial neural networks approach to stator current sensor faults detection for DTC-SVM structure", Power Electronics and Drives, vol.1(36), No.1, pp.128-138, 2016

[11] H. Ben Zina, M. Allouche, M. Souissi, M. Chaabane and L. Chrifi-Alaoui, "Robust Sensor Fault-Tolerant Control of Induction Motor Driver", International journal of Fuzzy Systems, vol.19, No.1, pp.155-166, 2017.

[12] S. Abderazak and N. Farid, "Comparative study between Sliding mode controller and Fuzzy Sliding mode controller in a speed control for doubly fed induction motor", Proceedings of the 4th International Conference on Control Engineering & Information Technology, Hammamet, Tunisia, pp.1-6, 2016.

[13] A. Fatima, T. Almas, M. A. K. A. Biabani and M. Imran, "Sliding mode control of induction motor used in traction", Proceedings of the International Conference on Electrical, Electronics and Optimization Techniques, Chennai, India, pp.3336-3343, 2016.

[14] M. El Azzaoui, H. Mahmoudi, C. Ed-dahmani and K. Boudaraia, "Comparing performance of PI and Sliding Mode in control of grid connected doubly fed induction generator", Proceedings of the International Renewable and Sustainable Energy Conference, Marrakech, Morroco, pp.769-774, 2016

[15] M. El Azzaoui, H. Mahmoudi, B. Bossoufi and M. El Ghamrasni, "Comparative study of the sliding mode and backstepping control in power control of a doubly fed induction generator", Proceedings of the International

Symposium on Fundamentals of Electrical Engineering, Bucharest, Romania, pp.1-5, 2016.

.

[16] S. Dandan, D. Yugang and Z. Chengning, "Sliding Mode Controller for Permanent Magnetic Synchronous Motors", Energy Procedia, vol.105, pp.2641-2646, 2017.

[17] T. Ameid, A. Menacer, H. Talhaoui, I. Harzelli and A. Ammar, "Backstepping control for induction motor drive using reduced model in healthy state: Simulation and experimental study", Proceedings of the 6th International conference on systems and control, Batna, Algeria, pp.162-167, 2017.

[18] H. Echeikh, R. Trabelsi, A. Iqbal, N. Bianchi and M. F. Mimouni, "Comparative study between the rotor flux oriented control and non-linear backstepping control of a five-phase induction motor drive-an experimental validation", IET Power Electronics, vol.9, No.13, pp.2510-2521, 2016.

[19] H. Echeikh, R. Trabelsi, A. Iqbal, N. Bianchi and M. F. Mimouni, "Non-linear backstepping control of five-phase IM drive at low speed conditions-experimental implementation", ISA transactions, vol.65, pp.244-253, 2016.

[20] H. Echeikh, R. Trabelsi, A. Iqbal, M. F. Mimouni and R. Alammari, "Online Adaptation of Rotor Resistance based on Sliding Mode Observer with Backstepping Control of A Five-Phase Induction Motor Drives", International Journal of Power Electronics and Drive Systems, vol.7, No.3, pp.648-655, 2016.

[21] N. Bouchiba, A. Barkia, S. Sallem, L. Chrifi-Alaoui, S. Drid and M. B. A. Kammoun, "A real-time Backstepping control strategy for a doubly fed induction generator based wind energy conversion system", Proceedings of the 6th International Conference on Systems and Control, Batna, Algeria, pp.549-554, 2017.

[22] H. Amimeur, D. Aouzellag, R. Abdessemed and K.Ghedamsi, "Sliding mode control of a dual-stator induction generator for wind energy conversion systems", International Journal of Electrical Power & Energy Systems, vol.42, No.1, pp.60-70, 2012.

[23] H. Amimeur, R. Abdessemed, D. Aouzellag, K. Ghedamsi, F. Hamoudi and S. Chekkal, "A sliding mode control for dual-stator induction motor drives fed by matrix converters", J Eletric Eng, vol.11, No.2, pp.136-143, 2011.

[24] H. Amimeur, R. Abdessemed, D. Aouzellag, E. Merabet and F. Hamoudi, "A sliding mode control associated to the field-oriented control of dual-stator induction motor drives", J Electr Eng, vol.10, No.3, pp.7-12, 2010.

[25] S. Lekhchine, T. Bahi, I. Abadlia and H. Bouzeria, "PV-battery energy storage system operating of asynchronous motor driven by using fuzzy sliding mode control", International Journal of Hydrogen Energy, vol.42, No.13, pp.8756-8764, 2017.

[26] E. E. M. Mohamed, M. A. Sayed, T. A. Ahmed and M. M. Hamada, "Position control of linear induction motor using cascaded sliding mode controller", Proceedings of the Eighteenth International Middle East Power Systems conference, Cairo, Egypt, pp.617-624, 2016.

[27] R. Trabelsi, A. Khedher, M. F. Mimouni and F. M'sahli, "Backstepping control for an induction motor using an adaptive sliding rotor-flux observer", Electric Power Systems Research, vol.93, pp.1-15, 2012.

AUTHOR PROFILES

N. Layadi was born in Bordj-Bou-Arreridj, Algeria. He received his Engineer degree in Automatic from Setif University and Master Diploma in Automatic from BBA University in 1998 and 2015, respectively. He is a PhD student in Electrical Engineering at the University of M'sila since 2016.

S. Zeghlache was born in Setif, Algeria. He received his Engineer degree in Automatic from M'sila University, Algeria, in 2006 and the Magister Diploma from Military Polytechnic School, -Bordj el Bahri- Algiers, Algeria, in 2009, all in Electrical Engineering. In 2011, he joined M'sila University-Algeria, where he works currently as lecturer. His research interests are non linear system control.

F. Berrabah was born in M'sila, Algeria, on June 13, 1979. He received the degrees of Engineer and Magister on electromechanical Engineering from Badji-Mokhtar Annaba, University Algeria in 2004 and 2009 respectively. He is a lecturer at University of M'sila Algeria. His research interests are mainly in the area of electrical drives and power electronics. He has authored and co-authored many conference papers.

L. Bentouhami received his under-graduate and Magister degrees in Electrical Engineering from M'sila and Batna universities in Algeria in 2004 and 2010, respectively. He is currently a PhD candidate at Batna University, his research interests are simulation and control of multi-phase induction machine.